Structure–Property Relationships for Sulfonated Poly(butylene terephthalate)

Bret J. Chisholm,* William D. Richards, Timothy E. Banach,† Sofia Soloveichik, James F. Kelley, Greg R. Bradtke, Sandeep Dhawan

GE Global Research Center, Niskayuna, New York 12309

Received 11 March 2005; accepted 22 September 2005
DOI 10.1002/app.23302
Published online in Wiley InterScience (www.interscience.wiley.com).

ABSTRACT: Structure–property relationships have been developed for sulfonated poly(butylene terephthalate) copolymers. The compositional variables investigated were sulfonate content, molecular weight, and polymer endgroup composition, and the fundamental polymer properties evaluated were melt viscosity, crystallization kinetics, and impact strength. It was found that all compositional variables significantly affect all of the polymer properties of interest. The most interesting effect is the influence of polymer endgroup composition on polymer properties. The trends indicate that the carboxylic acid endgroups form intermolecular interactions with sodium sulfonate groups, resulting in a decrease in the strength of intermolecular ionic interactions between sodium sulfonate groups. © 2006 Wiley Periodicals, Inc. J Appl Polym Sci 100: 4762–4771, 2006

Key words: plastics; ionomers; polyesters

INTRODUCTION

Poly(1,4-butylene terephthalate) (PBT) has become a very important semicrystalline thermoplastic for injection-molding applications. The strengths of PBT as an engineering thermoplastic resin are its excellent melt processability, fast crystallization, and good mechanical properties.

Our search for new materials with unique physical properties led us to study the modification of PBT by sodium sulfonate groups (Fig. 1). The level of sodium sulfonate groups of the copolymers of interest was less than 10 mol %. Therefore, they are considered members of the class of polymers referred to as ionomers.[1,2] For this class of materials, it is well known that the ion pairs, in an ionomer, aggregate together to form quadruplets, sextuplets, and higher aggregates, collectively called multiplets. The most widely accepted model for ionic aggregation in ionomers is the Eisenberg–Hird–Moore (EHM) model.[2] This model is based on the results obtained for polystyrene–carboxylate ionomers. The average size of the multiplets for these polystyrene ionomers, which are believed to contain only ionic material, was estimated to be about 6 Å in diameter, with an average of about five ion pairs per multiplet. The EHM model also describes a region of the polymer surrounding the multiplets called as "the region of restricted mobility." This region is comprised of polymer chain segments emanating from ion pairs in the multiplet, which, as a consequence of being tethered to the multiplet, possess lower segmental mobility than does polymer chain segments present in the nonionic matrix. The region of restricted mobility for polystyrene–carboxylate ionomers was estimated to be 10 Å thick.

It has been shown by many investigators that the presence of ionic functionality in semicrystalline polymers can have dramatic affects on polymer properties, such as melt viscosity (MV), crystallization rate, toughness, and solubility.[1] While considerable effort has gone into the study of semicrystalline ionomers, such as polyethylene ionomers[1] and syndiotactic polystyrene ionomers,[3,4] very little work has been reported on the properties of PBT ionomers (PBTIs).[5–7] The objective of the work described in this document was to develop structure–property relationships, relating the compositional variables of PBTIs to the polymer properties.

EXPERIMENTAL

Melt polymerization

A melt polymerization process was used to produce relatively low molecular weight PBTI precursors, from which higher molecular weight samples were subsequently prepared by solid state polymerization. A representative melt polymerization is as follows: 125.9 lb

Correspondence to: B. J. Chisholm (bret.chisholm@ndsu.edu).
**Present address:* Center for Nanoscale Science and Engineering, North Dakota State University, Fargo, ND 58102.
†*Present address:* Schenectady International, Inc., Schenectady, NY 12309.

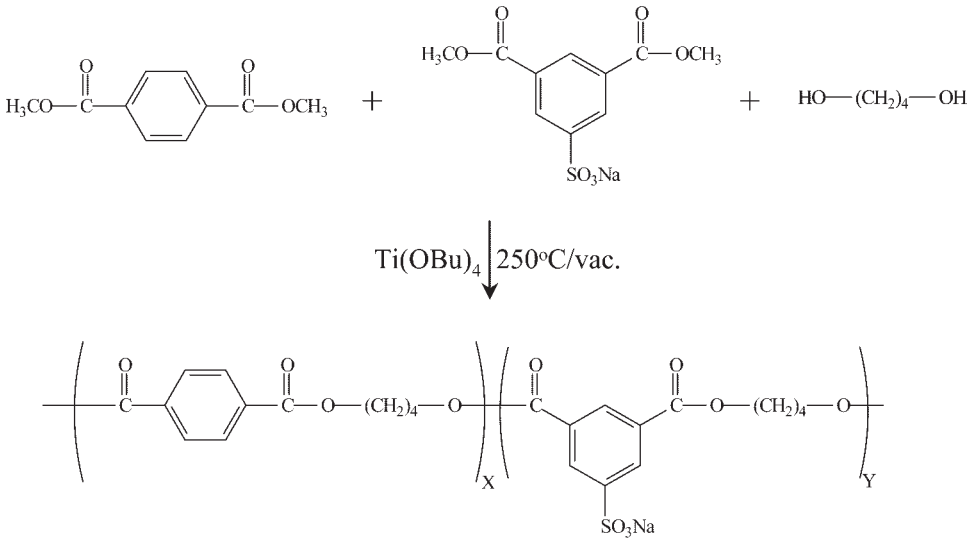

Figure 1 Schematic of the synthesis of PBTIs.

of dimethylterephthalate, 5.94 lb of dimethyl-5-sodiosulfo-1,3-phenylene dicarboxylate, 100 lb of 1,4-butanediol, and 43 mL of tetraisopropyl titanate were charged to a 40CV Helicone reactor that was preheated to 130°C. The monomer mixture was then heated to 225°C at a rate of 1.5°C/min under atmospheric pressure, and most of the methanol byproduct was removed by distillation. The mixture was then subjected to a gradual reduction in pressure at a rate of 20 mmHg/min while the temperature was simultaneously increased to 250°C at a rate of 1.5°C/min. After 132 min under vacuum, the first half of the batch (B1) was released from the reactor and chopped into granules. The remaining half of the batch (B2) was held in the reactor for 20 more minutes without vacuum, before it was removed and chopped into granules. The MV of B1 measured at 250°C and a shear rate of 100/s was 2400 poise, while the MV of B2 was 2300 poise. The carboxylic endgroup concentration for B1, measured by potentiometric titration, was 44 mequiv/kg, while the carboxylic endgroup concentration for B2 was 82 mequiv/kg.

Solid state polymerization

Higher molecular weight PBTI samples were prepared from low molecular weight PBTI precursors using solid-state polymerization. The precursors prepared by melt polymerization were in the form of chips. As a result, each sample was extruded using a 1 ¼ in. Welex single screw extruder, to ensure homogeneity and to obtain uniform-sized pellets for the solid-state polymerization.

A 50-L, glass-lined reactor, equipped with an agitator and a hot oil heater, was used for the solid-state polymerization. The reactor was purged with hot nitrogen to facilitate the heating of the pellets and the removal of 1,4-butanediol, the product of the condensation reaction. To perform the solid-state polymerizations, the reactor was charged with 20 lb of pellets, and then heated to ~210°C with oil and nitrogen. The reactions were monitored by periodically removing a small quantity of pellets for molecular weight analysis, as determined by carboxylic acid and hydroxyl endgroup measurements. When the desired low, intermediate, and high molecular weights were reached, 5 lb samples were removed from the reactor. These samples were then used without further modification.

Injection molding

Molded specimens for impact testing were injection molded using a 85 ton Van Dorn molding machine, with a barrel set temperature of 260–265°C, 65°C mold temperature, 10 s injection time, 20 s hold time, and 100 ψ back pressure. Pellets were dried at 87–93°C in a convection oven for 3 h, prior to molding.

Polymer endgroup determination

Similar to PBT, the endgroup composition of PBTIs was expected to be almost entirely a mixture of primary hydroxyl groups and aromatic carboxylic acid groups. Carboxylic acid endgroup concentration ([COOH]) was determined by potentiometric titration with tetrabutylammonium hydroxide, while hydroxyl endgroup concentration ([OH]) was determined by Fourier transfer infrared spectroscopy, using an adaptation of the method developed by Ward,[8] which involved recording spectra by subtracting a D_2O-exchanged reference film to remove overtones from the region of interest. The standard curve was constructed

TABLE I
Description of the Low Molecular Weight Polymers Used to Produce the Samples of Interest

Precursor ID	[SO_3Na] (mole %)	[COOH] (mequiv/kg)	[OH] (mequiv/kg)	M_n (g/mole)
3%–10.4K-44	3	44	149	10,400
3%–12.3K-83	3	83	73	12,300
1%–13.9K-41	1	41	99	13,900
3%–12.3K-39	3	39	122	12,300
1%–14.1K-79	1	79	64	14,100
5%–12.4K-50	5	50	111	12,400
5%–13.5K-86	5	86	64	13,500
3%–11.7K-63	3	63	109	11,700
3%–12.1K-80	3	80	86	12,100

using ^{1}H NMR spectroscopy instead of combustion analysis. The ^{1}H NMR spectra were recorded using long relaxation delays (25 s) to ensure accurate measurements, and over a range of samples with hydroxyl end group concentrations greater than those measured in this study.

From the endgroup composition, the number average molecular weight was calculated as follows:

$$M_n = 2 \times 10^6/([\text{OH}] + [\text{COOH}]) \quad (1)$$

where [OH] and [COOH] are expressed as milliequivalents/kg (mequiv/kg).

Materials

Eight low molecular weight PBTIs of varying ionic content and carboxyl endgroup concentration were prepared by melt polymerization. The ionic content, endgroup analyses, and molecular weights of these samples are listed in Table I.

Each of the PBTIs listed in Table I were solid-state polymerized to nominal molecular weights of 15,000, 18,000, and 21,000 g/mol. The measured [COOH] concentrations and M_n for each sample used in the study are provided in Table II. The values for the two commercially available PBTs (Valox® 195 and 315 from GE Plastics), which were used as reference materials, are also included in the table. Replicate materials for the three molecular weights at 3% ionic content and low [COOH] were produced and the corresponding data included in Table II.

Rheological measurements

Capillary and dynamic rheological measurements were performed on each sample in the study. All of the rheological measurements were conducted at 250°C. For both the capillary and dynamic rheological measurements, the samples were dried prior to testing for a minimum of 16 h at 110°C in a vacuum oven.

The capillary viscosity measurements were performed using a Goettfert 2002 rheometer equipped with a 30 × 1 mm^2 die and a 1000 bar pressure transducer. Viscosity values were determined over a shear rate range of 2500 and 10 s^{-1}. The apparent viscosities at shear rates of 1000 and 100 s^{-1} were used as characteristic values for further evaluation.

The dynamic rheological properties were measured using a Rheometrics RDS 7700 dynamic spectrometer, equipped with 25 mm diameter parallel plates and a nitrogen-purged environmental oven. The samples were prepared for testing by compression molding 1.0 in. diameter disks in a closed mold, using powdered resin obtained by grinding ~50 g of pellets. Because the dynamic measurements require only a small amount of material, the use of the powdered resin sample helped to ensure that a homogeneous and representative sample would be tested. Measurements were made over a frequency range of 0.1–400 rad/s, and complex viscosity values at 0.25 and 100 rad/s were used as characteristic values for evaluation. An indication of the melt stability of each sample was obtained by repeating the frequency sweep on the sample, after it had been held at 250°C for ~10 min. The relative stability was then calculated as follows:

$$\%|\eta^*| \text{ change} = \left(\frac{|\eta^*|_{\text{after 10 min}} - |\eta^*|_{\text{initial}}}{|\eta^*|_{\text{initial}}}\right) \times 100 \quad (2)$$

TABLE II
Description of the PBTIs Used for the Investigation

Sample ID	[SO_3Na] (mole %)	M_n (g/mole)	[COOH] (mequiv/kg)
Valox 195	0	14,600	19
Valox 315	0	37,600	38
1%–15.9K-40	1.0	15,900	40
1%–19.4K-37	1.0	19,400	37
1%–22.2K-38	1.0	22,200	38
1%–15.2K-80	1.0	15,200	80
1%–18.2K-78	1.0	18,200	78
1%–20.9K-74	1.0	20,900	74
3%–15.2K-43	3.0	15,200	43
3%–15.6K-42	3.0	15,600	42
3%–17.2K-48	3.0	17,200	48
3%–18.3K-47	3.0	18,300	47
3%–21.2K-49	3.0	21,200	49
3%–22.0K-50	3.0	22,000	50
3%–16.1K-63	3.0	16,100	63
3%–16.6K-63	3.0	16,600	63
3%–20.3K-64	3.0	20,300	64
3%–14.9K-82	3.0	14,900	82
3%–17.9K-81	3.0	17,900	81
3%–21.7K-78	3.0	21,700	78
5%–15.3K-55	5.0	15,300	55
5%–18.0K-59	5.0	18,000	59
5%–22.8K-61	5.0	22,800	61
5%–15.8K-88	5.0	15,800	88
5%–16.7K-90	5.0	16,700	90
5%–19.2K-92	5.0	19,200	92

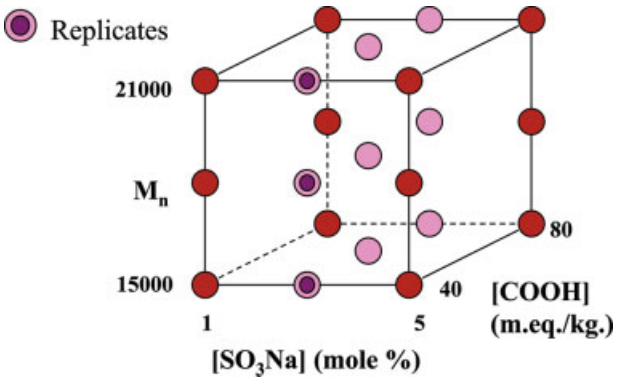

Figure 2 Schematic of the experimental design used for the study. [Color figure can be viewed in the online issue, which is available at www.interscience.wiley.com.]

For all these rheological tests, at least two tests were performed, and the average value was used in the analysis.

MV measurements were also performed on all the samples. MV is a viscosity control test for commercial Valox resins. The test is performed with a Melt Indexer at 250°C, using a 21.6 kg weight and a standard orifice (0.615 in. length × 0.042 in. diameter). The MV is calculated from the measured flow rate at these conditions.

Crystallization characteristics

Crystallization temperature was determined using differential scanning calorimetry (DSC). The instrument was a Perkin–Elmer® DSC 7 and was calibrated using an indium standard. The crystallization temperature (T_c) was reported as the minimum in the crystallization exotherm produced by cooling 3.0–4.5 mg specimens, cut from 0.5 to 2.0 mm thick, melt-pressed films from the melt at a rate of 40°C/min. The exact heating and cooling profile used is as follows: (1) heat from 30 to 265°C at 40°C/min; (2) hold at 265°C for 4.0 min; (3) cool from 265 to 30°C at 40°C/min; (4) hold at 30°C for 4.0 min; (5) heat from 30 to 250°C at 40°C/min. In addition to measuring the peak crystallization temperature, the heat of crystallization (ΔH_c) was measured by integrating the area of the crystallization exotherm. The crystallization temperatures and heats of crystallization, reported in this document, are all averages of three independent measurements.

Notched Izod impact strength

Notched Izod impact strength (NI) was measured on injection-molded specimens, using a 5 lb hammer. The impact strengths reported in this document are all averages of 10 measurements.

RESULTS AND DISCUSSION

The polymer compositional variables for PBTIs are molecular weight (M_n), ionic content ([SO_3Na]), and acid endgroup concentration ([COOH]). The fundamental polymer properties considered in this study

TABLE III
Rheological Properties at 250°C for the Samples Prepared

Sample ID	MV (Pa s)	$\|\eta^*\|$ at 0.25 rad/s (Pa s)	$\|\eta^*\|$ at 100 rad/s (Pa s)	η_{app} at 100 s^{-1} (Pa s)	η_{app} at 1000 s^{-1} (Pa s)
Valox 195	700	1,260	1,310	860	760
Valox 315	8,500	11,600	8,830	8,610	4,350
1%–15.9K-40	4,250	5,890	4,820	4,210	2,360
1%–19.4K-37	8,730	13,200	8,730	7,570	3,380
1%–22.2K-38	12,800	21,300	11,700	11,400	4,300
1%–15.2K-80	1,790	2,350	2,200	1,830	1,310
1%–18.2K-78	3,770	4,080	3,540	3,460	2,090
1%–20.9K-74	5,470	6,410	5,040	5,190	2,750
3%–15.2K-43	12,000	25,600	12,500	11,900	4,070
3%–15.6K-42	10,400	21,000	11,100	9,850	3,630
3%–17.2K-48	18,600	41,700	16,300	17,300	5,150
3%–18.3K-47	17,500	45,200	17,200	16,700	5,000
3%–21.2K-49	23,800	83,100	23,500	23,600	—
3%–22.0K-50	22,300	73,800	22,100	22,100	6,940
3%–16.1K-63	8,650	15,700	9,340	8,860	3,430
3%–16.6K-63	11,100	19,600	10,800	10,700	3,880
3%–20.3K-64	14,400	38,900	16,200	15,400	4,700
3%–14.9K-82	8,510	13,000	8,130	8,130	3,390
3%–17.9K-81	14,300	25,100	12,300	13,600	4,430
3%–21.7K-78	16,200	28,800	13,100	14,600	4,670
5%–15.3K-55	14,100	27,900	13,500	14,200	4,440
5%–18.0K-59	18,500	44,600	17,700	18,600	5,230
5%–22.8K-61	23,500	105,000	26,900	28,400	7,920
5%–15.8K-88	11,200	15,300	9,110	10,600	3,830
5%–16.7K-90	12,600	20,100	11,000	12,300	4,230
5%–19.2K-92	17,500	35,200	15,300	17,100	5,040

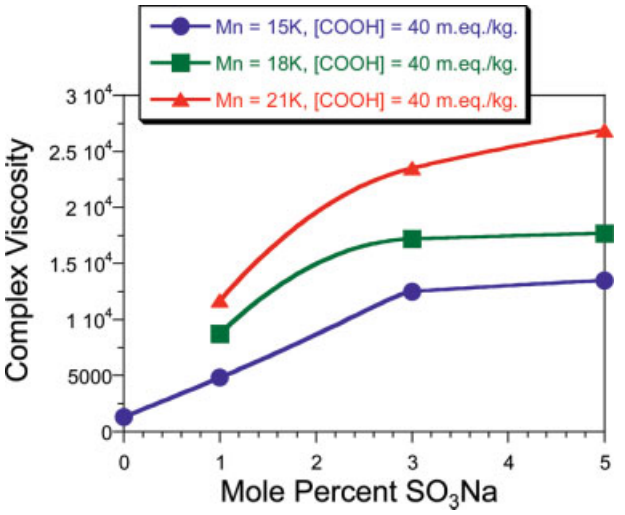

Figure 3 η^* at 100 rad/s (Pa s) for the PBTI samples investigated, illustrating the effect of [SO_3Na] and molecular weight. [Color figure can be viewed in the online issue, which is available at www.interscience.wiley.com.]

include the rheological properties, thermal properties, and impact strength. The experimental design used for the study is illustrated in Figure 2. The [SO_3Na] and [COOH] limits were chosen to cover as broad a compositional range as practical. The lower limit for the M_n was chosen to be approximately the same as that of the lowest molecular weight of the PBT control (Valox 195). The upper M_n limit was the highest that could be attained while still maintaining the high [COOH]. Three replicate compositions were included in the design to estimate error.

Rheological properties

The characteristic rheological properties for each sample are listed in Table III. The results for η^* at 100 rad/s as a function of PBTI composition are shown graphically in Figures 3 and 4. The general trends observed for η^* at 100 rad/s are consistent with those of the other rheological properties measured. PBTI viscosity is strongly dependent on all three compositional variables. It increases as M_n and [SO_3Na] increase, and decreases as [COOH] increases. Over the compositional space evaluated, η^* at 100 rad/s varies more than an order of magnitude.

The dependence of MV on molecular weight has been well documented.[1] The effect of ionic content on MV of ionomers is also known.[1,3] The ionic associations persist in the melt, acting as transient crosslinks that increase the resistance to flow. The effect of acid endgroups on ionomer MV is less well known. The trend between MV and [COOH] suggests that the acid endgroups interact with the sodium sulfonate groups on the backbone to weaken the intermolecular ionic associations, and thereby increasing molecular mobility.[9,10] Acid endgroups, thus, counteract the effect of the ionic species on the rheological properties of PBTI.

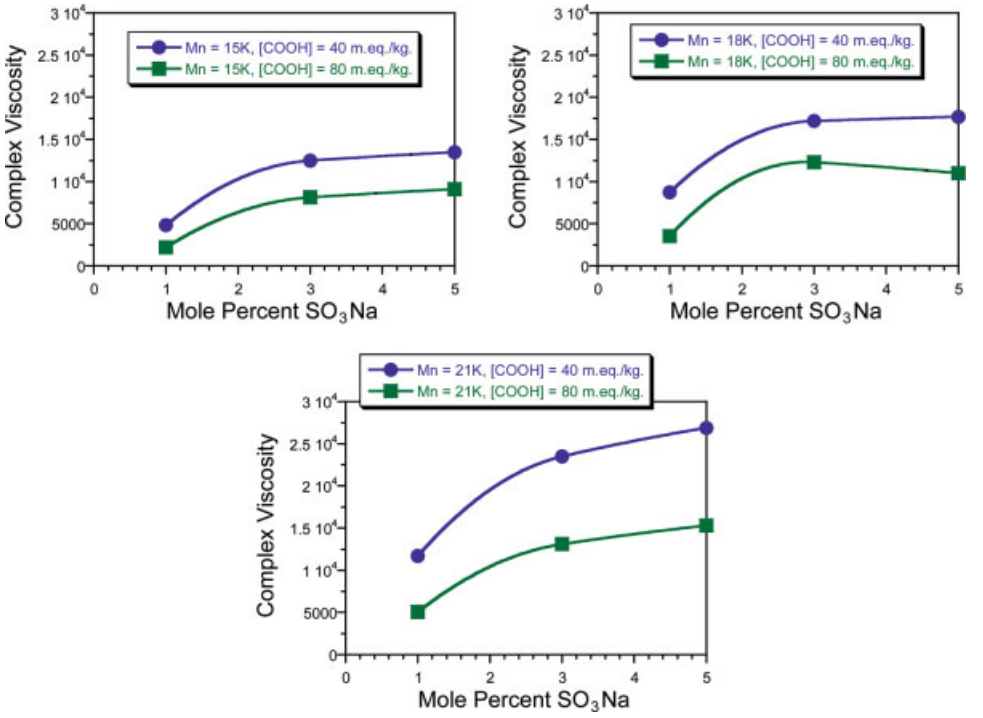

Figure 4 Plots illustrating the effect of [COOH] on complex viscosity. [Color figure can be viewed in the online issue, which is available at www.interscience.wiley.com.]

TABLE IV
Correlation Results between the Different Viscosity Measurements

Correlation parameters	$\|\eta^*\|$ at 100 rad/s *vs.* MV	η_{app} at 100 s^{-1} *vs.* MV	η_{app} at 100 s^{-1} *vs.* $\|\eta^*\|$ at 100 rad/s
Slope	0.950	0.985	1.006
Intercept	167	−202	−16
R	0.978	0.995	0.988

There is an excellent correlation between the MV, η^* at 100 rad/s, and η_{app} at 100 s^{-1} data if the highest viscosity PBTI (5–22.8K-61) is excluded from the analysis. The linear coefficients and regression values are shown in Table IV. The equivalence of η^* at 100 rad/s and η_{app} at 100 s^{-1} as indicated by the near zero intercept and a slope of one in the linear regression, confirms the validity of the Cox–Merz[11] rule for these polymers:

$$|\eta^*|(\omega) = \eta(\gamma) \text{ at } \omega = \gamma \tag{3}$$

Melt stability

The melt stability values calculated for each sample are listed in Table V, and are shown graphically in Figure 5. Depending on the composition, the viscosity increases, remains relatively constant, or decreases with time. The largest increase in viscosity occurs when the M_n, [SO_3Na], and [COOH] are all low, and conversely, the largest decrease occurs when these parameters are all high. It appears that more than one process influences the melt stability.

TABLE V
Melt Stability for the Samples Prepared

Sample ID	%$\|\eta^*\|$ change at 0.25 rad/s	%$\|\eta^*\|$ change at 100 rad/s
Valox 195	38	21
Valox 315	−7	−6
1%–15.9K-40	25	4
1%–19.4K-37	11	0
1%–22.2K-38	3	−4
1%–15.2K-80	3	1
1%–18.2K-78	−1	−3
1%–20.9K-74	−6	−5
3%–15.2K-43	12	−5
3%–15.6K-42	11	−5
3%–17.2K-48	−4	−8
3%–18.3K-47	−6	−9
3%–21.2K-49	−14	−10
3%–22.0K-50	−14	−14
3%–16.1K-63	1	−5
3%–16.6K-63	−3	−7
3%–20.3K-64	−13	−10
3%–14.9K-82	−8	−7
3%–17.9K-81	−18	−12
3%–21.7K-78	−18	−11
5%–15.3K-55	−3	−9
5%–18.0K-59	−14	−11
5%–22.8K-61	−25	−14
5%–15.8K-88	−14	−11
5%–16.7K-90	−16	−11
5%–19.2K-92	−23	−14

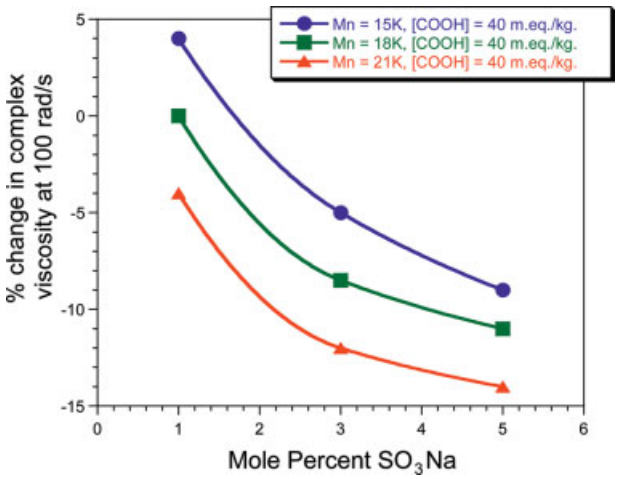

Figure 5 Melt stability measured at 100 rad/s for the PBTI samples investigated, illustrating the effect of [SO_3Na]. [Color figure can be viewed in the online issue, which is available at www.interscience.wiley.com.]

It is known that [COOH] increases with time for PBT and PBTI when held in the molten state.[7] This increase in [COOH] is due to the intramolecular reaction involving hydroxy-terminated chain ends.[12] An increase in [COOH] in the melt with time would result in disruption of the ionic associations and a subsequent decrease in viscosity. The rate of viscosity drop would be expected to be greatest for PBTIs with high [SO_3Na], where the initial viscosity was highest. Also, the likelihood of a newly formed acid endgroup finding an ionic association in its vicinity to disrupt would increase with increasing [SO_3Na].

The process leading to viscosity increases in low molecular weight PBTIs is quite likely the same as that for low molecular weight PBTs. As shown in Table V, Valox 195 increases significantly in viscosity in the melt. Previous studies with PBT stability indicate that this viscosity increase is due to associations developed between newly generated acid endgroups and the titanate catalyst.[13] The competition for the acid endgroups between the catalyst and ionic groups and their opposite effects on viscosity produces a rather complex melt stability behavior observed in the PBTIs.

Thermal properties

Table VI displays the T_c data obtained in the study. Each T_c is an average of the three measurements. In general, the data shows the following trends: (1) increasing [SO_3Na] at a given M_n and [COOH] decreases the T_c (Fig. 6); (2) increasing M_n at a given [SO_3Na]

TABLE VI
Thermal Property Data Obtained for the Samples Prepared

Sample ID	T_c (°C)	ΔH_c (J/g)
Valox 195	190.0	52.5
Valox 315	182.5	50.4
1%–15.9K-40	178.5	47.6
1%–19.4K-37	176.3	45.8
1%–22.2K-38	174.5	45.2
1%–15.2K-80	181.2	49.5
1%–18.2K-78	180.3	48.9
1%–20.9K-74	179.8	47.2
3%–15.2K-43	170.0	46.8
3%–15.6K-42	169.6	46.2
3%–17.2K-48	168.0	45.1
3%–18.3K-47	166.7	45.0
3%–21.2K-49	166.6	43.7
3%–22.0K-50	165.6	43.2
3%–16.1K-63	173.2	47.1
3%–16.6K-63	173.2	46.5
3%–20.3K-64	171.4	45.3
3%–14.9K-82	171.8	47.4
3%–17.9K-81	170.7	46.3
3%–21.7K-78	170.9	45.3
5%–15.3K-55	160.3	44.9
5%–18.0K-59	156.9	43.5
5%–22.8K-61	153.2	42.2
5%–15.8K-88	164.9	46.8
5%–16.7K-90	164.5	46.4
5%–19.2K-92	162.9	45.2

and [COOH] decreases T_c (Fig. 6); and (3) increasing [COOH] at a given [SO_3Na] and M_n increases T_c (Fig. 7).

The decrease in T_c obtained by increasing [SO_3Na] can be attributed to a decrease in the mobility of the polymer chains because of electrostatic ionic interactions, and the inability of the sulfonate comonomer unit to cocrystallize with PBT chain segments. A reduction in crystallization rate resulting from the incorporation of ionic functionality into a semicrystalline polymer has been observed by other investigators.[3,4]

In addition to reducing the rate of crystallization, the inability of the sulfonate comonomer units to cocrystallize with PBT chain segments results in a reduction in the melting point of PBTIs. Figure 8 shows the variation in melting temperature with [SO_3Na] for samples of similar M_n and [COOH], crystallized from the melt by cooling at 40°C/min. From the slope of the line shown in Figure 8, it was determined that, over the range of [SO_3Na] investigated, the experimental melting point decreases about 1.15°C/mole % of sodium sulfonate comonomer. For comparison purposes, the theoretical predictions of melting point depression for the PBTI samples can be made using the relationship derived by Flory[14]:

$$1/T_m^* - 1/T_m^0 = -R/\Delta H_u(\ln n) \quad (4)$$

This relationship was derived to describe the melting point depression resulting from random incorporation of noncrystallizable monomer units into a crystallizable backbone. T_m^0 (is the equilibrium melting point of the parent homopolymer (i.e., PBT), T_m^* (is the equilibrium melting point of the copolymer (i.e., PBTI), R is the gas constant, ΔH_u is the heat of fusion per mole of crystallizable units, and n is the mole fraction of crystallizable units. Using values obtained from literature for the T_m^0 (238°C)[15] and ΔH_u (31 kJ/mol)[16] of PBT, the melting point depression for PBT copolymers is calculated to be 0.70°C per mole of comonomer units. Considering the fact that melting points determined for the PBTI samples were not equilibrium melting points and, thus, cannot be directly compared to the theoretical predictions, the rate of change of the experimental melting point with [SO_3Na] is in good agreement with this theoretical prediction. This result indicates that the sulfonate comonomer units are not incorporated into the PBT crystalline lattice, and reside only in the amorphous phase.

The most interesting chemical structure—T_c interaction is the interaction between [COOH] and T_c. The COOH endgroups can interact or coordinate with sodium sulfonate groups through hydrogen bonding or acid–base interactions. These hydrogen bonding or acid–base interactions between —COOH endgroups and sodium sulfonate groups would be significantly weaker than the purely ionic interactions that would otherwise exist between sodium sulfonate groups. Thus, the effect of the —COOH/—SO_3Na interactions would be to reduce the overall strength of the ionic network, resulting in enhanced polymer chain mobility. An enhancement in polymer chain mobility provided by an increase in [COOH] is consistent with the decrease in MV and increase in T_c, observed for the PBTIs investigated.

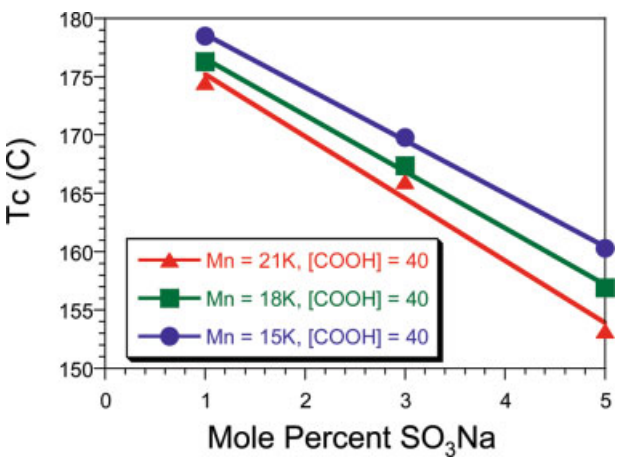

Figure 6 Illustration of the effect of [SO_3Na] and molecular weight on T_c. [Color figure can be viewed in the online issue, which is available at www.interscience.wiley.com.]

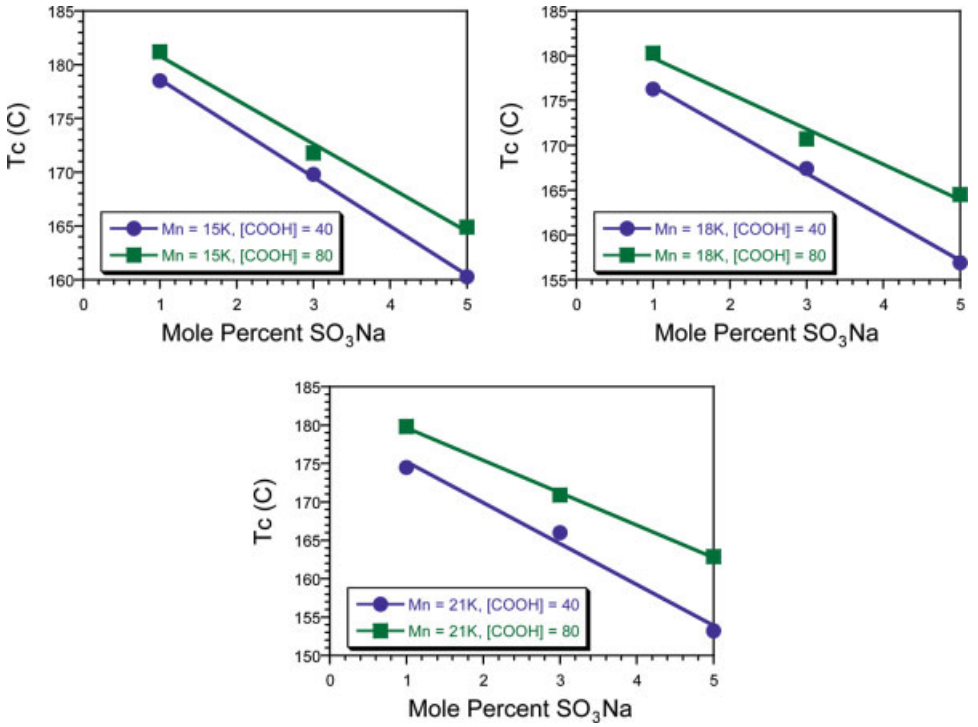

Figure 7 Plots illustrating the effect of [COOH] on T_c. [Color figure can be viewed in the online issue, which is available at www.interscience.wiley.com.]

Heat of crystallization

In addition to the peak of the crystallization temperature, T_c, the amount of heat liberated upon crystallization from the melt (ΔH_c) was determined. It is expected that the ΔH_c values would correlate with the level of crystallinity in injection-molded specimens. The general trends between ΔH_c and PBTI chemical composition are essentially the same as those obtained for T_c: (1) increasing the sodium sulfonate content at a given molecular weight and carboxylic acid content decreases ΔH_c; (2) increasing the molecular weight at a given sodium sulfonate content and carboxylic acid endgroup content decreases ΔH_c; and (3) increasing

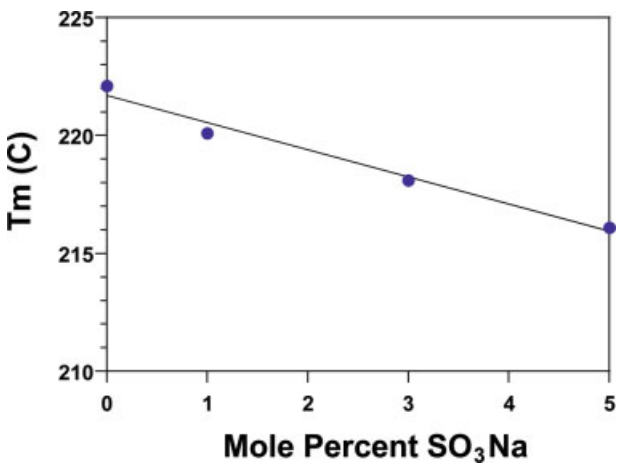

Figure 8 Illustration of the effect of [SO_3Na] and molecular weight on T_m. [Color figure can be viewed in the online issue, which is available at www.interscience.wiley.com.]

TABLE VII
Notched Izod Impact Strength Data

Sample ID	NI (ft lb/in.)
Valox 195	0.530
Valox 315	1.190
1%–15.9K-40	0.705
1%–19.4K-37	0.820
1%–22.2K-38	0.913
1%–15.2K-80	0.506
1%–18.2K-78	0.645
1%–20.9K-74	0.704
3%–15.2K-43	0.813
3%–15.6K-42	0.823
3%–17.2K-48	0.965
3%–18.3K-47	0.990
3%–21.2K-49	1.144
3%–22.0K-50	1.625
3%–16.1K-63	0.835
3%–16.6K-63	0.920
3%–20.3K-64	1.020
3%–14.9K-82	0.798
3%–17.9K-81	0.864
3%–21.7K-78	1.050
5%–15.3K-55	1.252
5%–18.0K-59	1.549
5%–22.8K-61	3.357
5%–15.8K-88	1.121
5%–16.7K-90	1.249
5%–19.2K-92	1.429

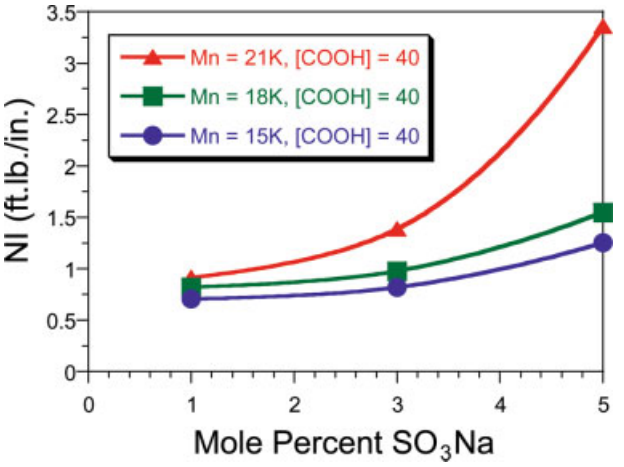

Figure 9 Illustration of the effect of [SO_3Na] and molecular weight on NI. [Color figure can be viewed in the online issue, which is available at www.interscience.wiley.com.]

the carboxylic acid endgroup content at a given sulfonate content and molecular weight increases ΔH_c. A correlation between T_c and ΔH_c is expected, since the ultimate level of crystallinity for a given cooling process would depend on T_c. The higher the T_c, the more time available for the crystallization process to take place, allowing for higher extents of crystallization to be achieved.

Notched izod impact strength

Table VII displays the NI data obtained. Each NI value is an average of 10 measurements. In general, the data displayed in Figure 9 show the following trends: (1) increasing the sodium sulfonate content at a given molecular weight and carboxylic acid content increases NI; (2) increasing the molecular weight at a given sodium sulfonate content and carboxylic acid endgroup content increases NI; and (3) increasing the carboxylic acid endgroup content at a given sulfonate content and molecular weight decreases NI (Fig. 10). It is noteworthy that the NI of many of the PBTI samples was significantly higher than that of the commercially produced Valox 315, even though the molecular weight of the Valox 315 is much higher than any of the PBTI samples. The NI of 3.357 ft lb/in. for sample 5%–22.8K-61 is three times higher than Valox 315 and is, in general, extremely high for any semicrystalline polymer.

The improvement in NI, obtained by the incorporation of sodium sulfonate groups into the polymer structure, may be due to changes in the viscoelastic properties of the material induced by the presence of ionic aggregates or to a reduction in the level of crystallinity of molded specimens because of the reduction in crystallization rate imparted by ionic associations in the melt. As noted in a review by Tant and Wilkes,[17] very little work has been reported on the mechanical properties of ionomers in the glassy state. Since molecular motions are restricted to short range molecular motion below T_g, it might be expected that the effect of ionic interactions would be small. However, some researchers have found interesting effects of ionic interactions on low-temperature sub-T_g transitions, sug-

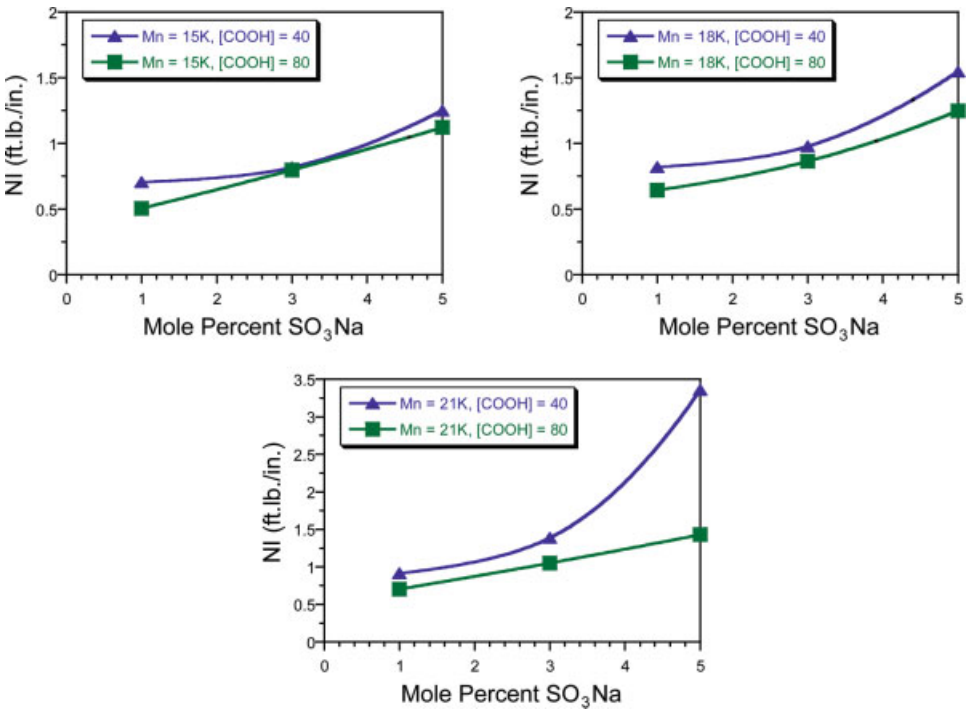

Figure 10 Illustration of the effect of [COOH] on NI. [Color figure can be viewed in the online issue, which is available at www.interscience.wiley.com.]

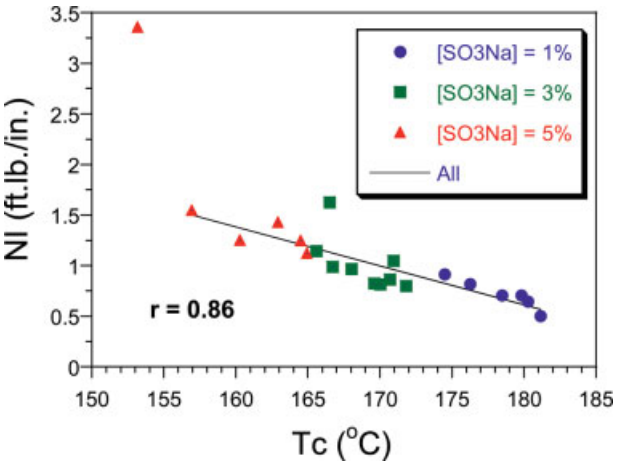

Figure 11 Correlation between NI and T_c. [Color figure can be viewed in the online issue, which is available at www.interscience.wiley.com.]

gesting that ionic interactions may affect the mechanical properties of ionomers in the glassy state.[18–20]

Since the ductility of a semicrystalline polymer can depend very strongly on the level of crystallinity of molded specimens, the NI data has been plotted as a function of the crystallization data, T_c and ΔH_c, to determine whether there is a correlation between the properties. As shown in Figure 11, excluding the data point for the PBT-ionomer possessing the lowest T_c, a good correlation exists between T_c and NI. The correlation between ΔH_c and NI is substantially poorer than that between T_c and NI, which may be due to the higher variability in the measurement of ΔH_c, resulting from the ambiguity in setting a baseline for peak area integration. The good correlation between T_c and NI suggests that the main mechanism of influence of chemical structure ([SO_3Na], M_n, and [COOH]) on NI is through the rate of development of crystallinity during the injection-molding process. Chemical structure features that a decrease in the rate of crystallization increases NI. This result suggests a good correlation between T_c and the level of crystallinity in an injection specimen. Unfortunately, the level of crystallinity of molded specimens was not measured to verify this correlation.

CONCLUSIONS

The results obtained from this study show that all three compositional variables ([SO_3Na], M_n, and [COOH]) strongly affect all of the properties evaluated. The most unique effect observed is the relationship between [COOH] and PBTI properties. This relationship suggests that COOH endgroups influence properties by interacting with SO_3Na groups, in a manner, that weakens the intermolecular ionic associations between SO_3Na groups. The weakened associations are evidenced by a drop in viscosity and impact, and by an increase in T_c.

References

1. Tant, M. R.; Mauritz, K. A.; Wilkes, G. L. Eds. Ionomers: Synthesis, Structure, Properties and Applications; Blackie: London, UK, 1997.
2. Eisenberg, A.; King, M. Ion-Containing Polymers: Physical Properties and Structure; Academic Press: New York, 1977.
3. Orler, E. B.; Calhoun, B. H.; Moore, R. B. Macromolecules 1996, 29, 5965.
4. Orler, E. B.; Yontz, D. J.; Moore, R. B. Macromolecules 1993, 26, 5157.
5. Gorda, K. R.; Peiffer, D. G. J Polym Sci Part B: Polym Phys 1992, 30, 281.
6. Chisholm, B. J.; Moore, R. B.; Barber, G.; Khouri, F.; Hempstead, A.; Larsen, M.; Olson, E.; Kelley, J.; Balch, G.; Caraher, J. Macromolecules 2002, 35, 5508.
7. Chisholm, B. J.; Sisti, L.; Soloveichik, S.; Gillette, G. Polymer 2003, 44, 1903.
8. Ward, I. M. Trans Faraday Soc 1957, 53, 1406.
9. Vanhoorne, P.; Register, R. Macromolecules 1996, 29, 598.
10. Ha, C. S.; Cho, Y. W.; Cho, W. J.; Kim, Y.; Inoue, T. Polym Eng Sci 2000, 40, 1816.
11. Cox, W. P.; Merz, E. H. J Polym Sci 1958, 28, 619.
12. Pilati, F.; Manaresi, P.; Fortunato, B.; Munari, A.; Passalacqua, V. Polymer 1981, 22, 1566.
13. Banach, T. E.; Richards, W. D. Unpublished results.
14. Flory, P. J. Principles of Polymer Chemistry; Cornell University Press: Ithaca, NY, 1953.
15. Chisholm, B. J.; Zimmer, J. G. J Appl Polym Sci 2000, 76, 1296.
16. Wunderlich, B.; Cheng, S. Z. D.; Loufakis, K. In Encyclopedia of Polymer Science and Engineering; Mark, H. F., Bikales, N. M., Overberger, C. G., Menges, G., Eds.; Wiley: New York, 1989; Vol. 16, p 767.
17. Tant, M. R.; Wilkes, G. L. In Ionomers: Synthesis, Structure, Properties and Applications; Tant, M. R., Mauritz, K. A., Wilkes, G. L., Eds.; Blackie: London, UK, 1997; p 265.
18. Drzewinki, M.; MacKnight, W. J. J Appl Polym Sci 1985, 30, 4753.
19. Hara, M.; Jar, P.; Sauer, J. A. Macromolecules 1988, 21, 3183.
20. Hara, M.; Jar, P. Y. Macromolecules 1988, 21, 3187.